



Supplement of

Upper-lithospheric structure of northeastern Venezuela from joint inversion of surface-wave dispersion and receiver functions

Roberto Cabieces et al.

Correspondence to: Roberto Cabieces (rcabdia@roa.es)

The copyright of individual parts of the supplement might differ from the article licence.

1. Histograms for data selection

This section shows the histograms and the Probability Density Functions of Rayleigh and Love wave dispersion measurements. The measurements outside three standard deviations have been rejected from the computation of the dispersion maps, being considered outliers.

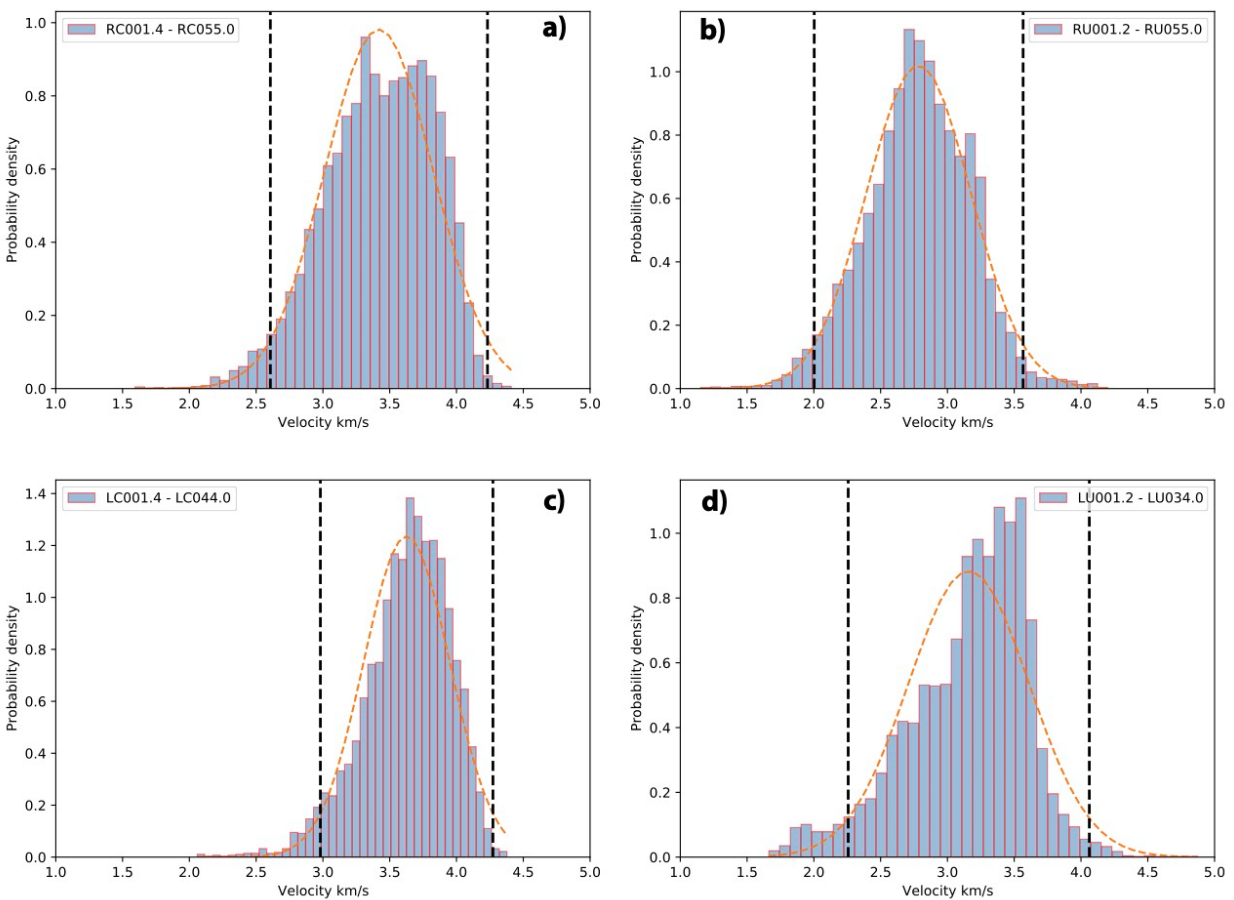


Fig S1. Histograms and Probability Density Functions (PDFs). Individual blue bins show the relative number of dispersion measures in a) and c) Rayleigh (RC) and love wave phase (LC) velocity, b) and d) Rayleigh (RU) and Love wave group (LU) velocity. Orange dashed lines are the best-fitting Gaussian PDFs and black dotted lines show the outlier limits set to three standard deviations.

2. Ray path coverage

2.1 Group Velocity (Rayleigh wave)

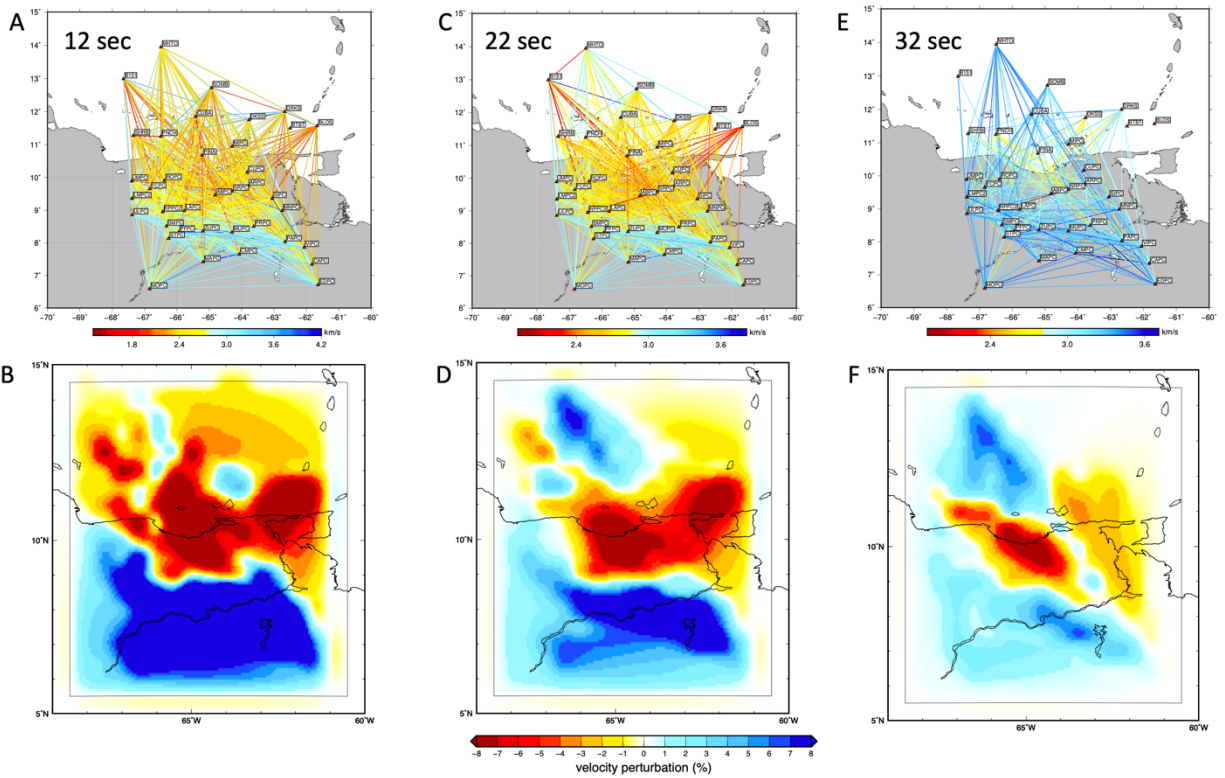


Figure S2. Rayleigh-wave ray-paths and group velocity maps for wave periods of 12, 22 and 32 seconds. Upper panels, A, C and E show ray-paths shaded according to the recorded velocities between pairs of stations. Lower panels, B, D and F correspond to group velocity maps for the wave periods shown in the above panel.

2.2 Phase Velocity (Rayleigh wave)

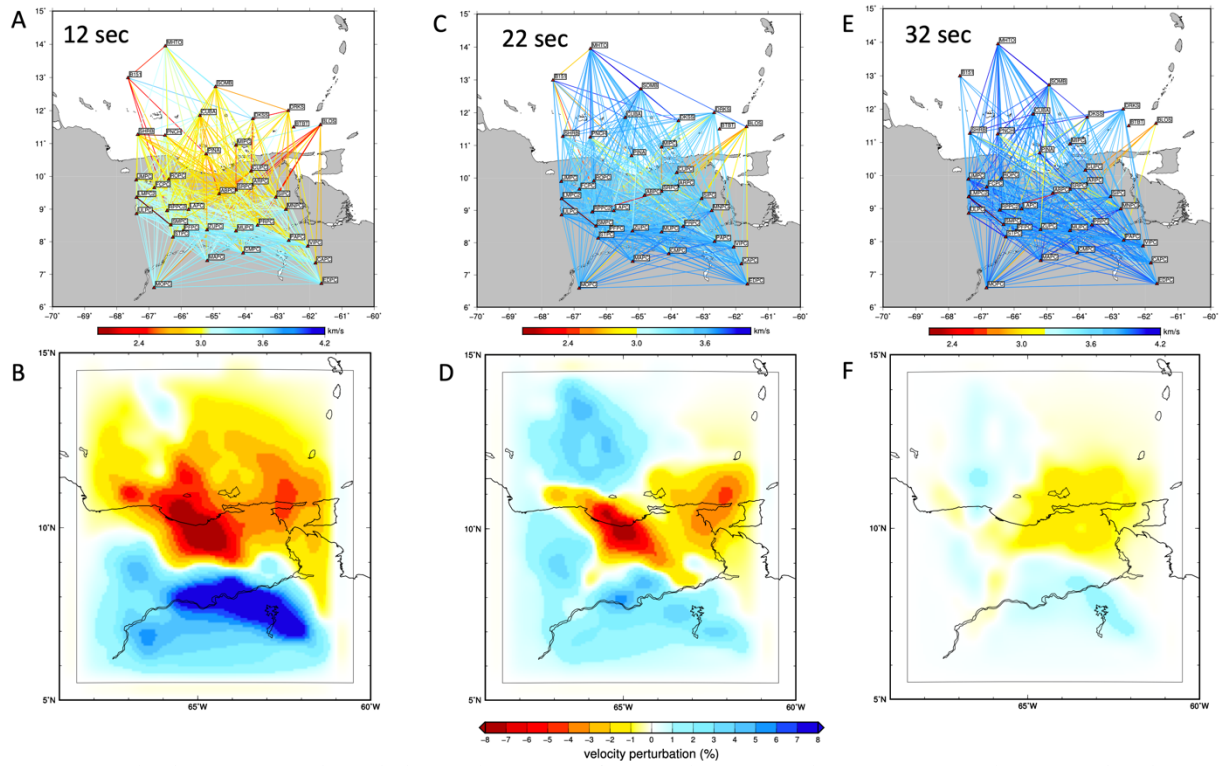


Figure S3. Rayleigh-wave ray-paths and phase velocity maps for periods 12, 22 and 32 s. Upper panels, A, C and E show ray-paths shaded according to the measured velocities between each station pair. Lower panels, B, D and F contain the phase velocity maps for the periods shown in the above panel.

2.3 Group Velocity (Love wave)

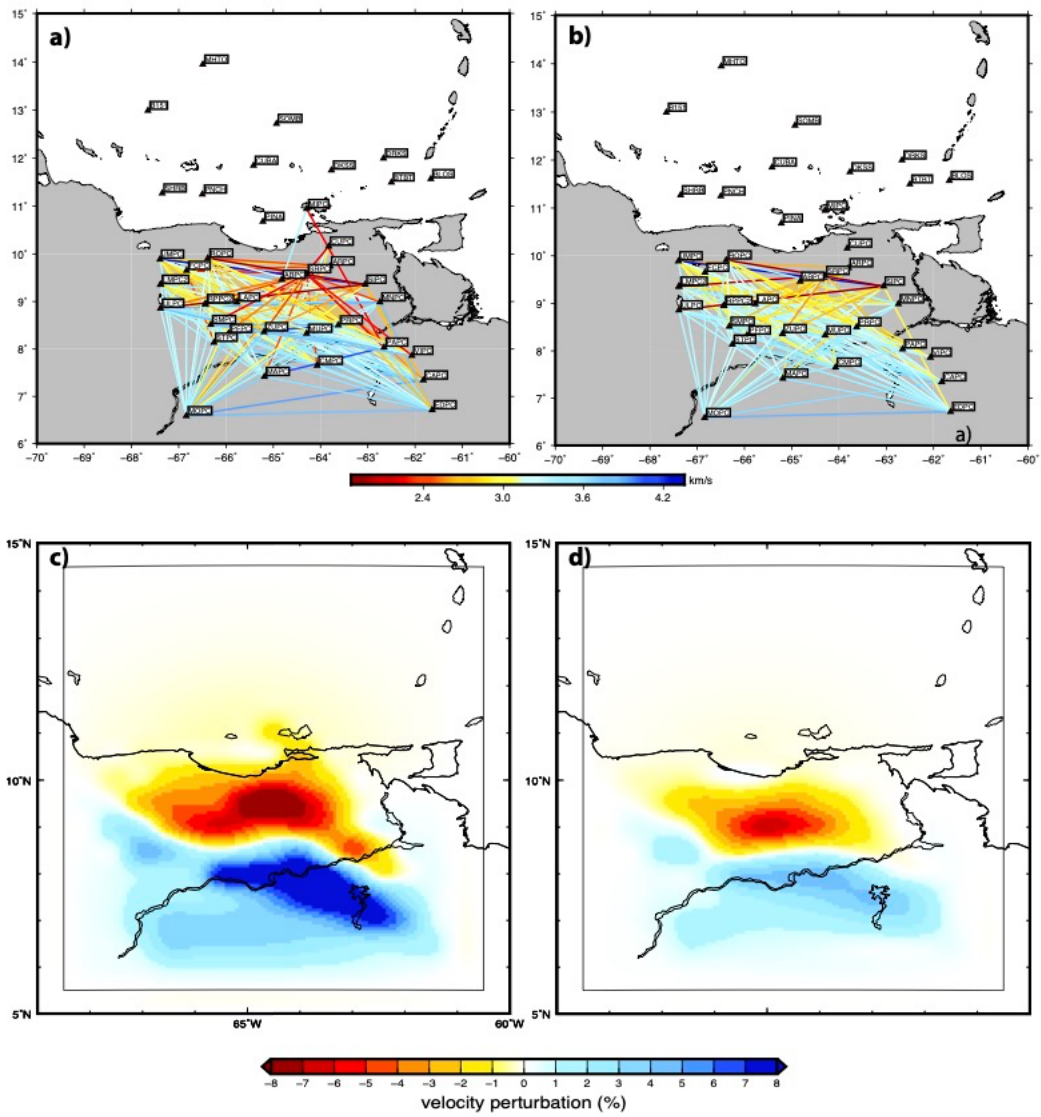


Figure S4. Love wave ray-paths and group velocity maps for periods 12 s (left) and 20 s (right). Upper panels a) and b) show ray-paths shaded according to the measured velocities between each station pair. Lower panels c) and d) contain the group velocity maps for the periods shown in the above panel.

2.4 Phase Velocity (Love wave)

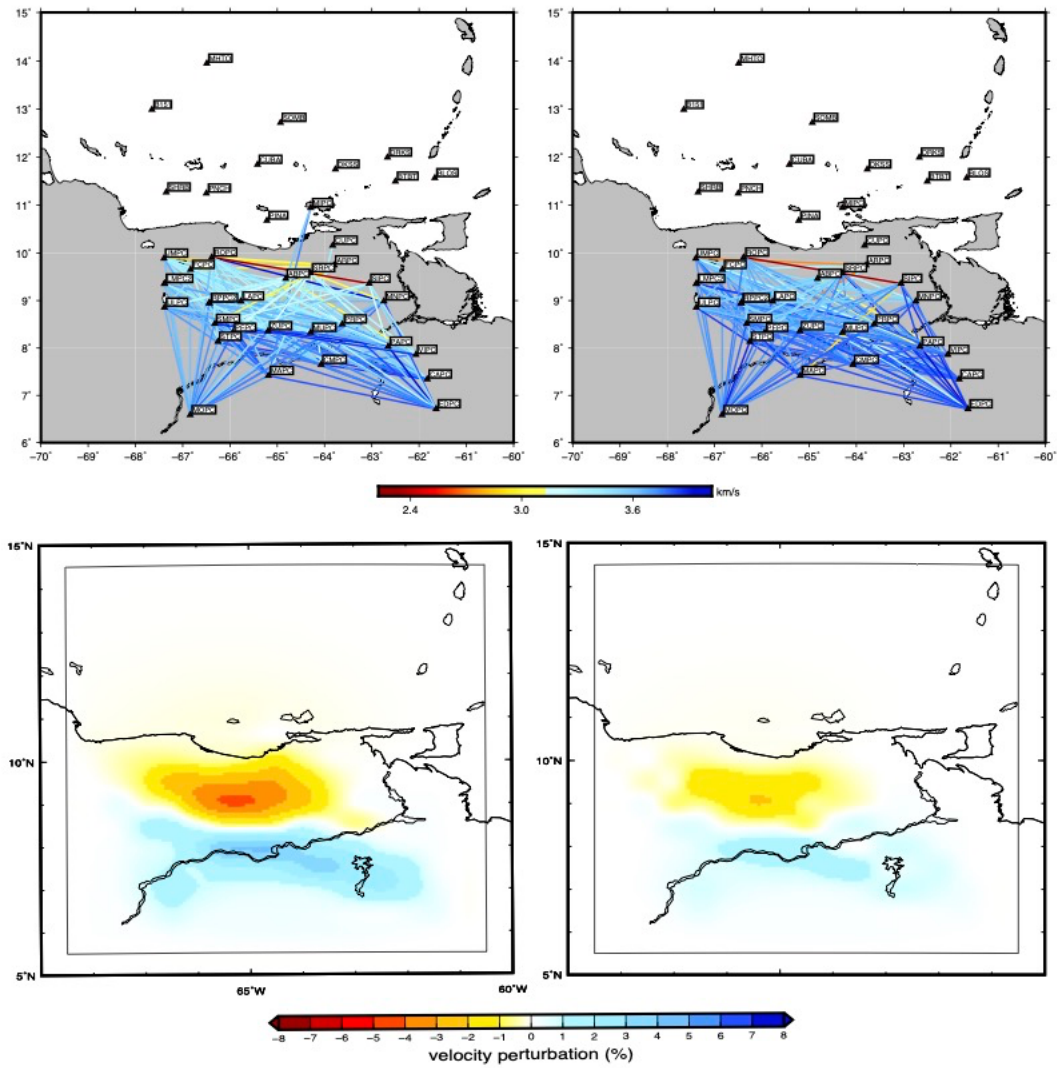


Figure S5. Love wave ray-paths and phase velocity maps for periods 12 s (left) and 20 s (right). Upper panels a) and b) show ray-paths shaded according to the measured velocities between each station pair. Lower panels c) and d) contain the phase velocity maps for the periods shown in the above panel.

3. Checkerboard tests

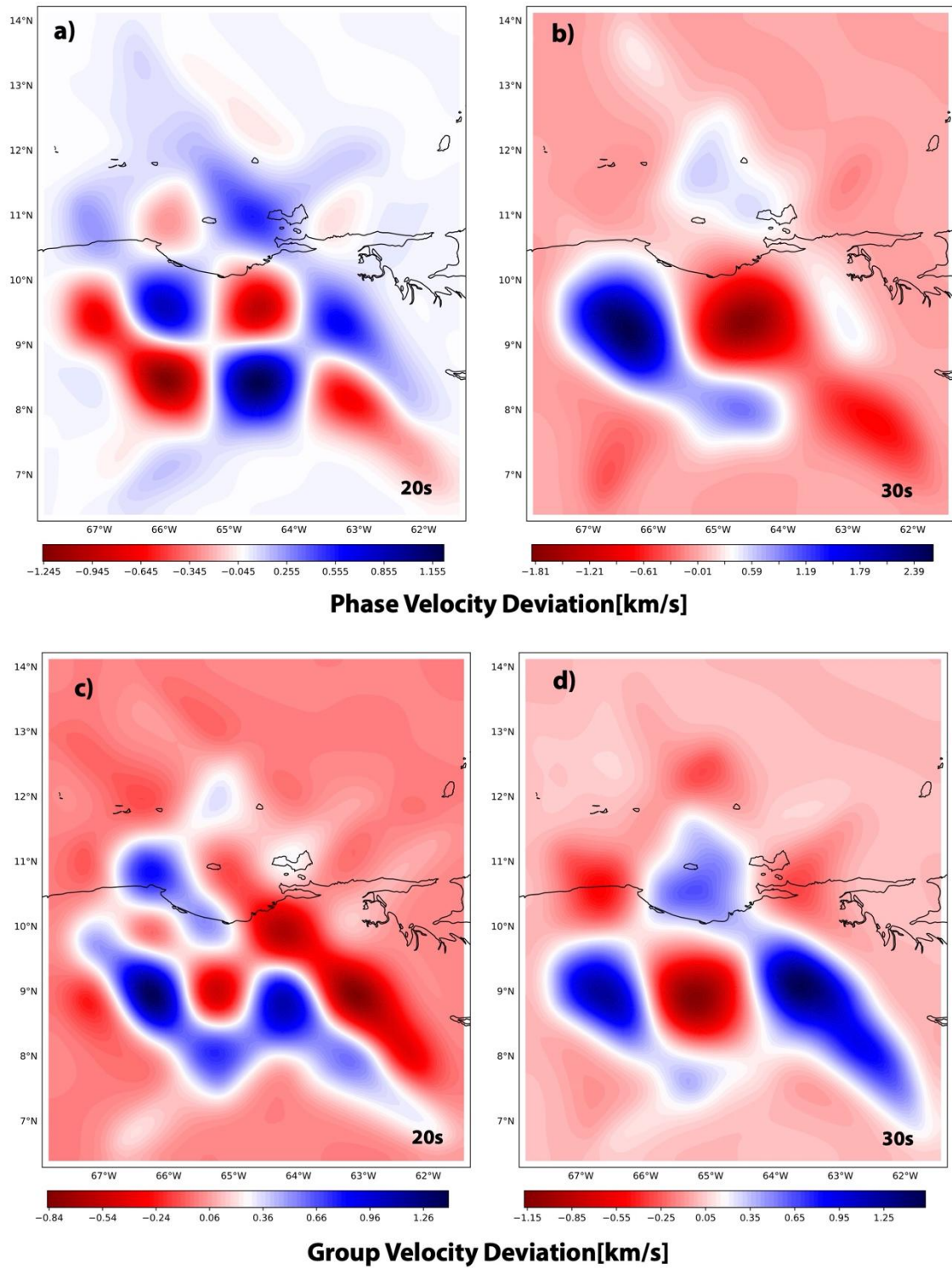
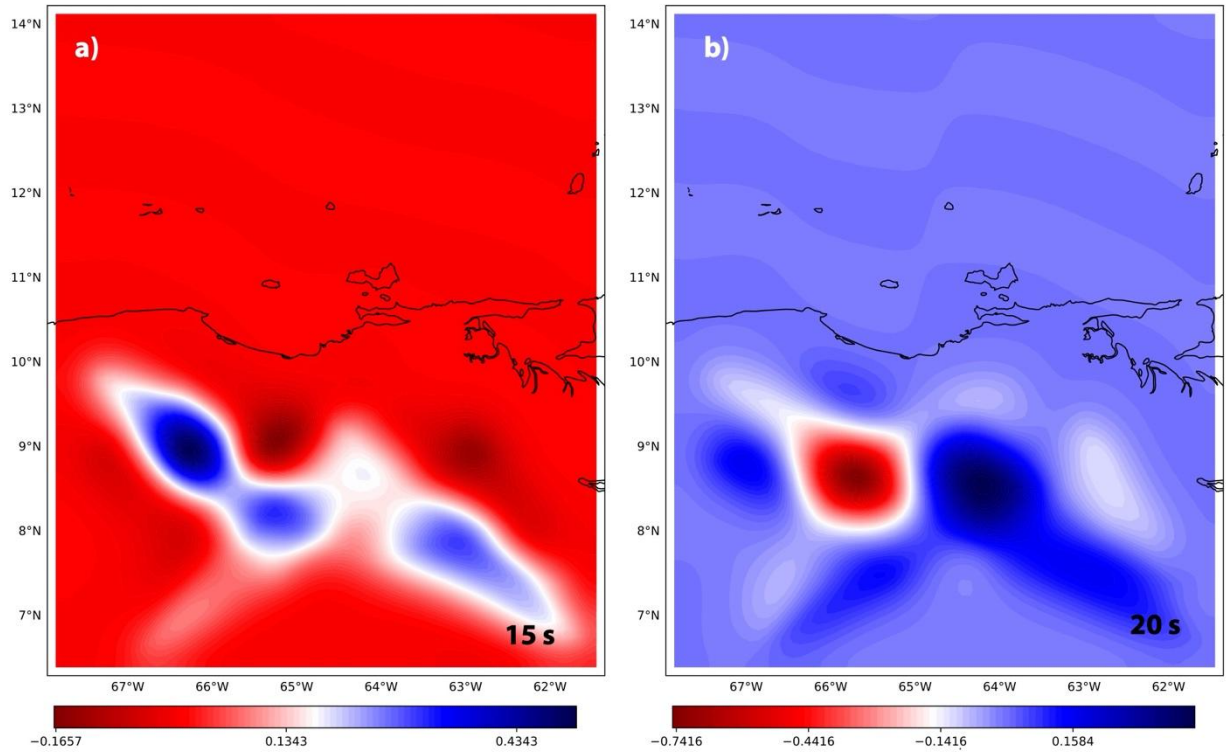
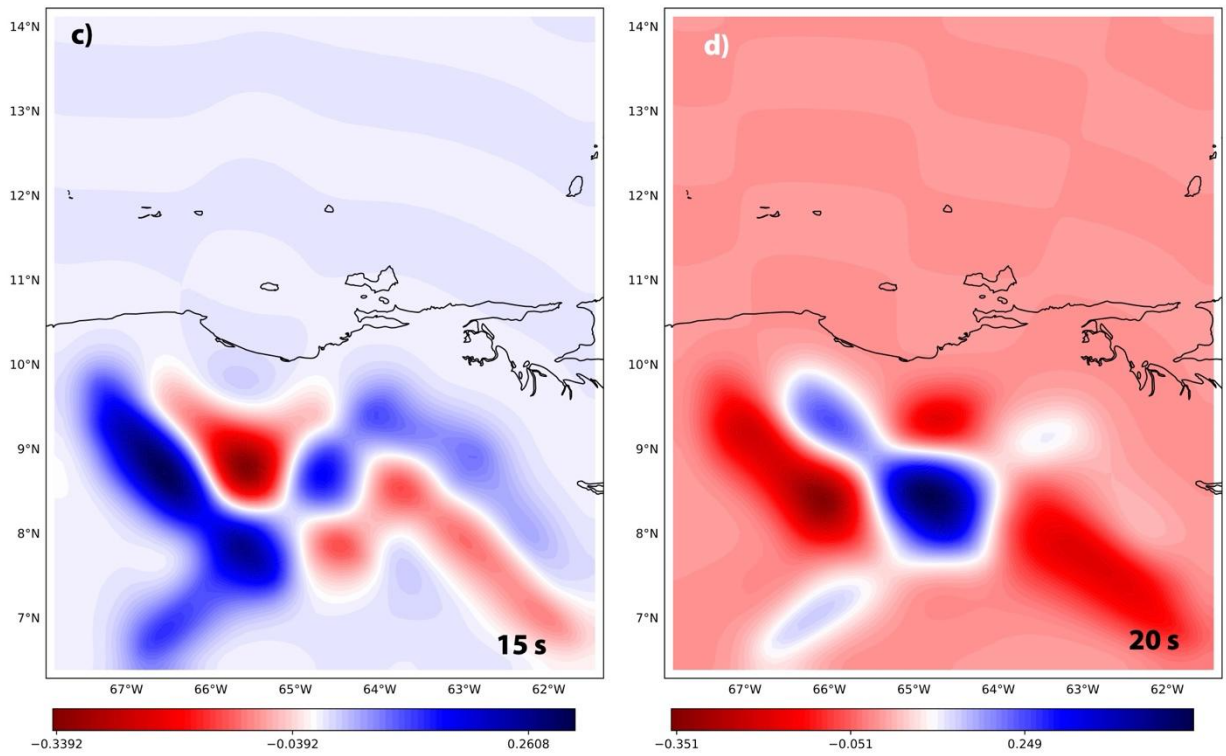


Figure S6. Checkerboard tests corresponding to the available Rayleigh wave data coverage for periods 20 and 30 s.



Phase Velocity Deviation [km/s]



Group Velocity Deviation [km/s]

Figure S7. Checkboard tests corresponding to the available Love wave data coverage for periods 15 and 20 s.

4. Resolution Maps

The spatial resolution maps were computed following the approach described by Barmin et al. (2001). First, the resolution matrix for the traveltime inverse problem is computed. Each row from the resolution matrix is tied to a geographical location in the phase/group velocity maps and can be interpreted as the velocity model that would be obtained if only a point anomaly existed in that geographic point (Goutorbe et al., 2015). A cone is then fitted to each row of the resolution matrix, and the radius of this cone is reported as the spatial resolution, i.e., the smallest sized anomaly that can be resolved.

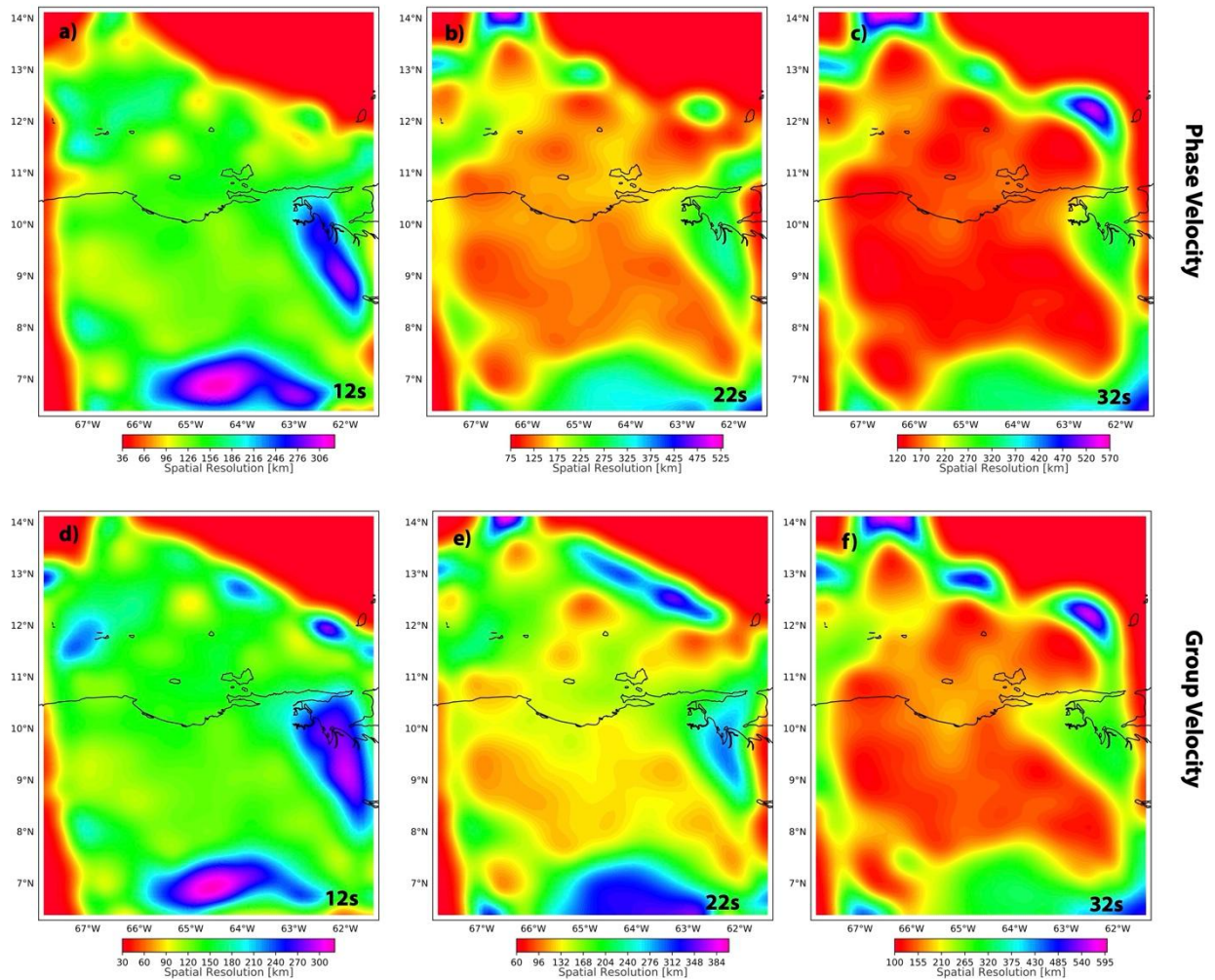


Figure S8. Resolution maps computed for the group and phase velocity maps of Rayleigh waves for 12 s (a and d), 22 s (b and e) and 32 s (c and f).

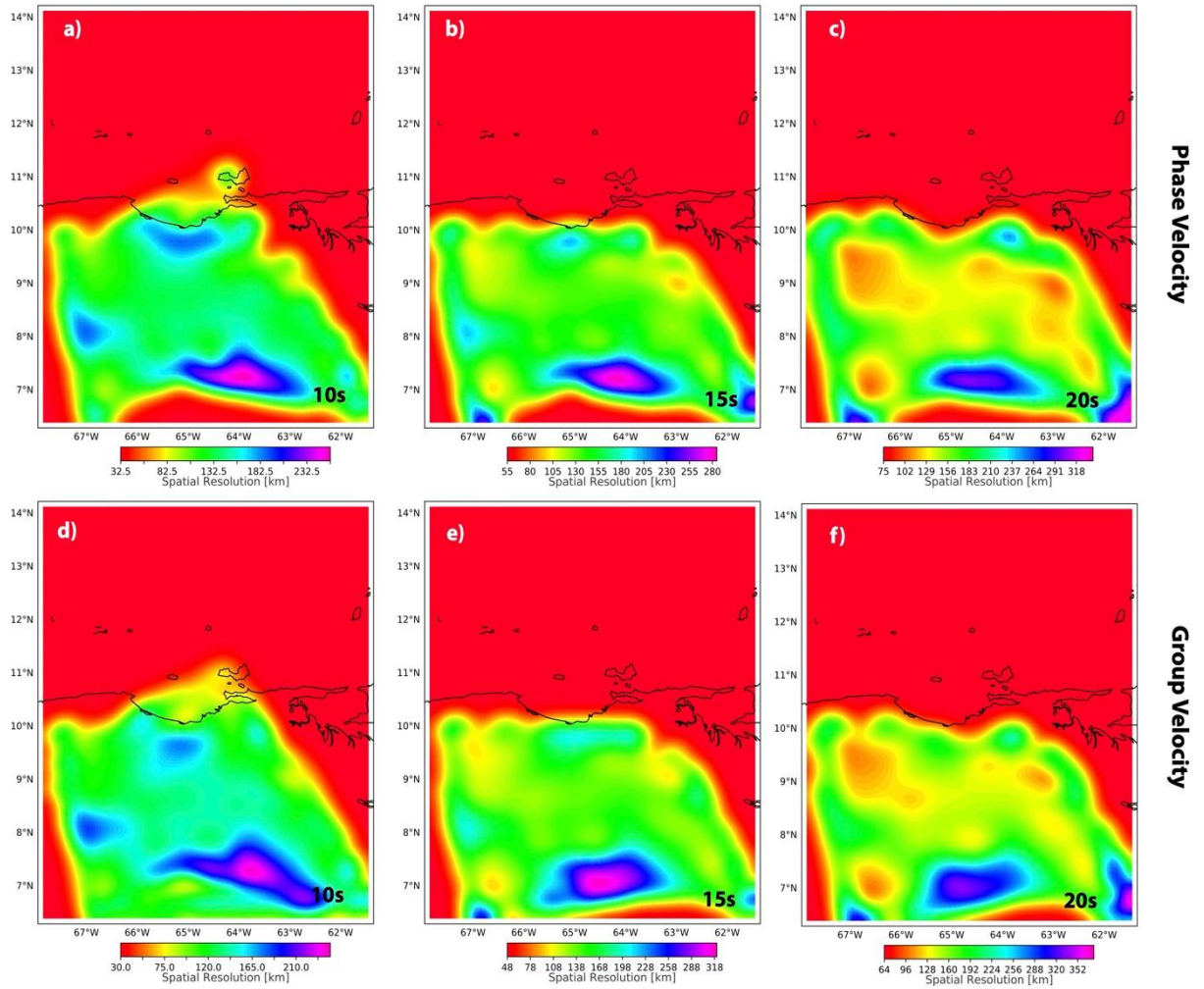


Figure S9. Resolution maps computed for the group and phase velocity maps of Love waves for 10 s (a and d), 15 s (b and e) and 20 s (c and f).

5. Stations Orientation

Table S1. Orientation values for the nominal north-component of the ocean bottom seismometers (OBS). The computation is briefly described in section 2.4 in the main text.

Station Name	Azimuth $^{\circ}$	Error $^{\circ}$ (2σ)
B151	257.5	3.0
BLOS	077.8	13.0
BTBT	-	-
CUBA	130.5	4.0
DKSS	201.1	8.0
MHTO	286.0	2.3
PINA	289.0	15.4
PNCH	176.1	4.2
SHRB	106.5	3.1
SOMB	227.3	3.5

6. Receiver Functions

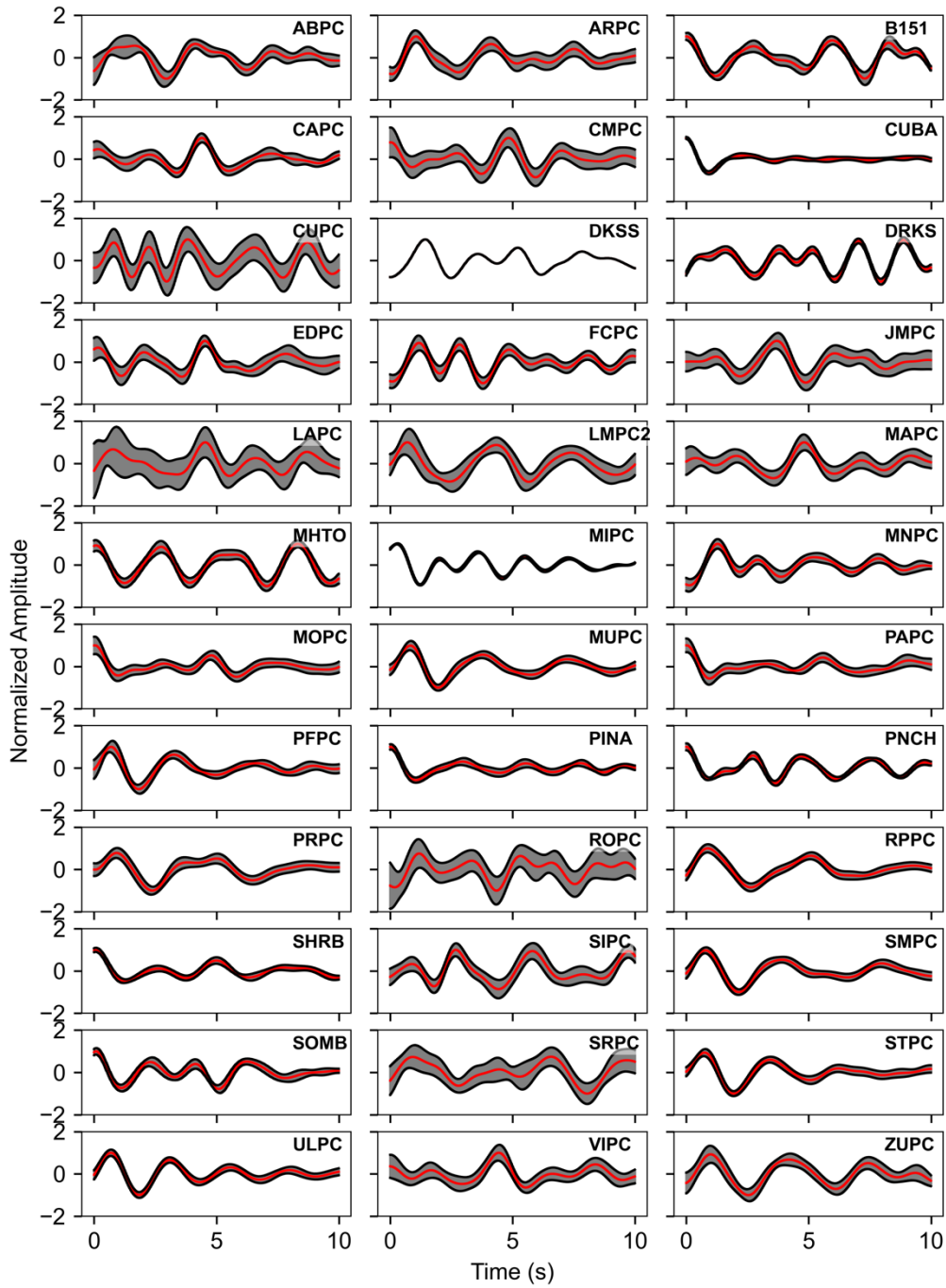


Figure S10. Isotropic receiver functions (red lines) computed for all land stations and ocean bottom seismometers used in the joint inversion. The shaded grey area shows the associated uncertainty.

7. Probability Density Plots

In this section we present Probability Density plots representing the V_s posterior distribution and interface probabilities, from a random selection of 2500 models per chain obtained from a total number of chains of 40 and a total number of μ models of 100000). Blue line represents the mode, red line the mean and green line the median of the V_s posterior distribution for different depths.

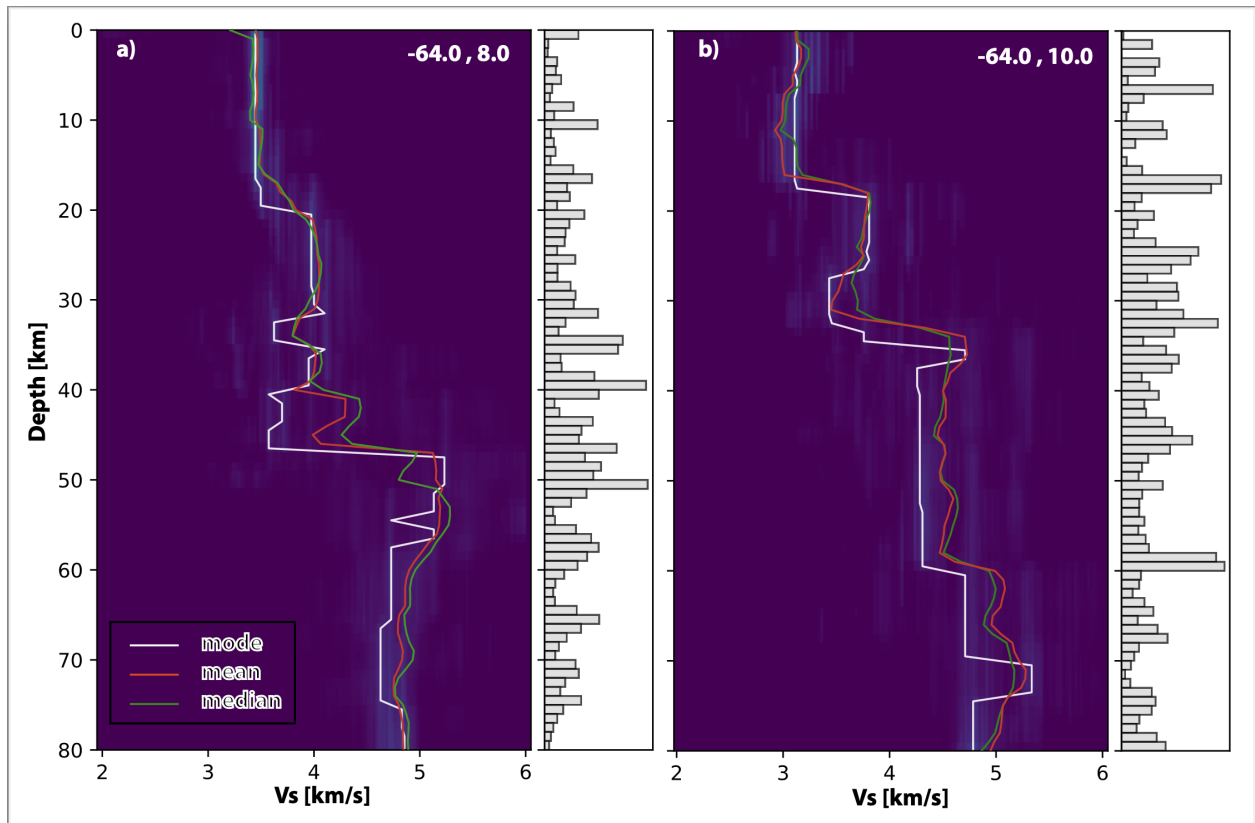


Figure S11. V_s posterior distributions and interface depth probabilities. a) Results obtained for the geographic location $64.0^\circ W$, $8.0^\circ N$, white line the mode, red line the mean and green line the median from the ensemble of the best models. b) same as a) but for the geographic location $-64.0^\circ W$, $10.0^\circ N$. Histograms show probability of interface depth.

8. Moho map from 3D Vs model

In addition to performing H-k stacking of receiver functions (see main text), we also estimated Moho depths from the nearest (distance $< 0.5^\circ$) 1D Vs models to the stations and interpolating through the neighboring algorithm to the rest of the studied region.

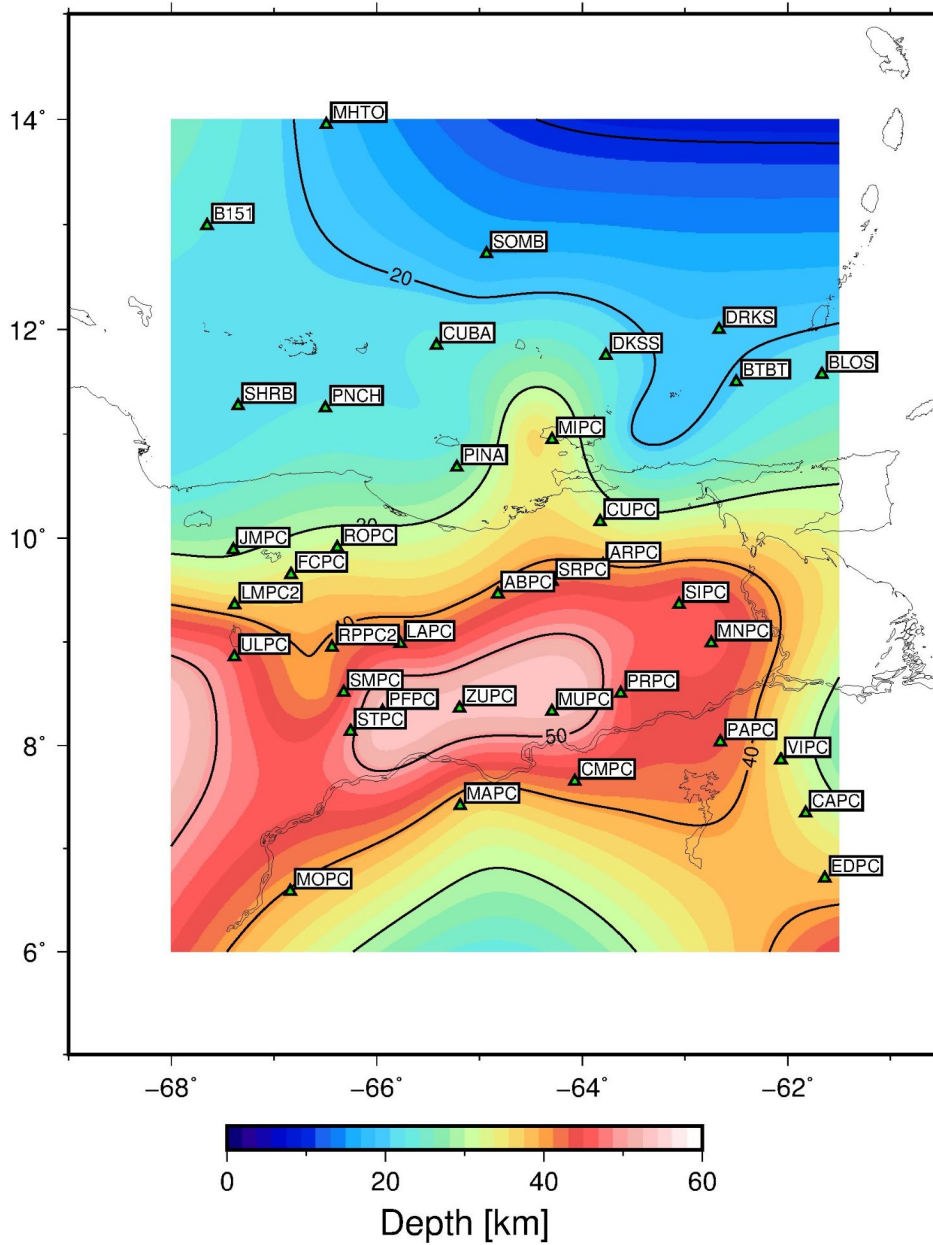


Figure S12. Map of the Moho depth estimation through the interpolation of Vs 1D models. Green Triangles show the stations used to estimate the Moho depth. Contour lines every 20 km for the Moho depth.

9. Uncertainty Maps

This section presents 2D uncertainty maps (standard deviation in V_s) for the same depths as in Fig 11.

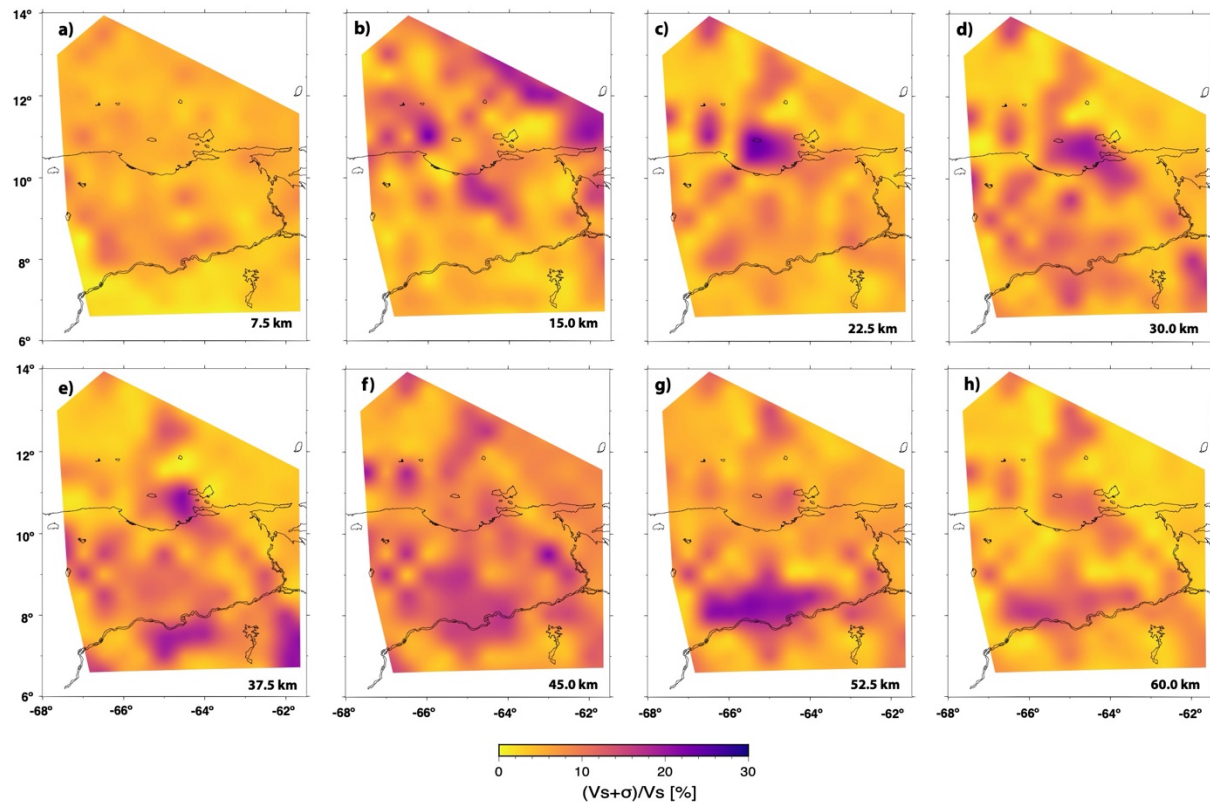


Figure S13. Horizontal slices of the standard deviation associated to the 3D shear wave velocity model obtained in this study. From a) to h) increasing depth in steps of 7.5 km until 60 km. depth. VB (Venezuela Basin), GS (Guayana Shield), MB (Maturin Basin), GB (Guarico Basin), SI (Serrania del Interior), TB (Turtle the Island-Barcelona Bay) and PoP (Peninsula of Paria).

10. Vs model anomalies

Vs model anomalies map shows the percentual perturbations between our model (V_s) and the global 1-D model (V_m) ak-135 (Kennett et al., 1995), for different depths.

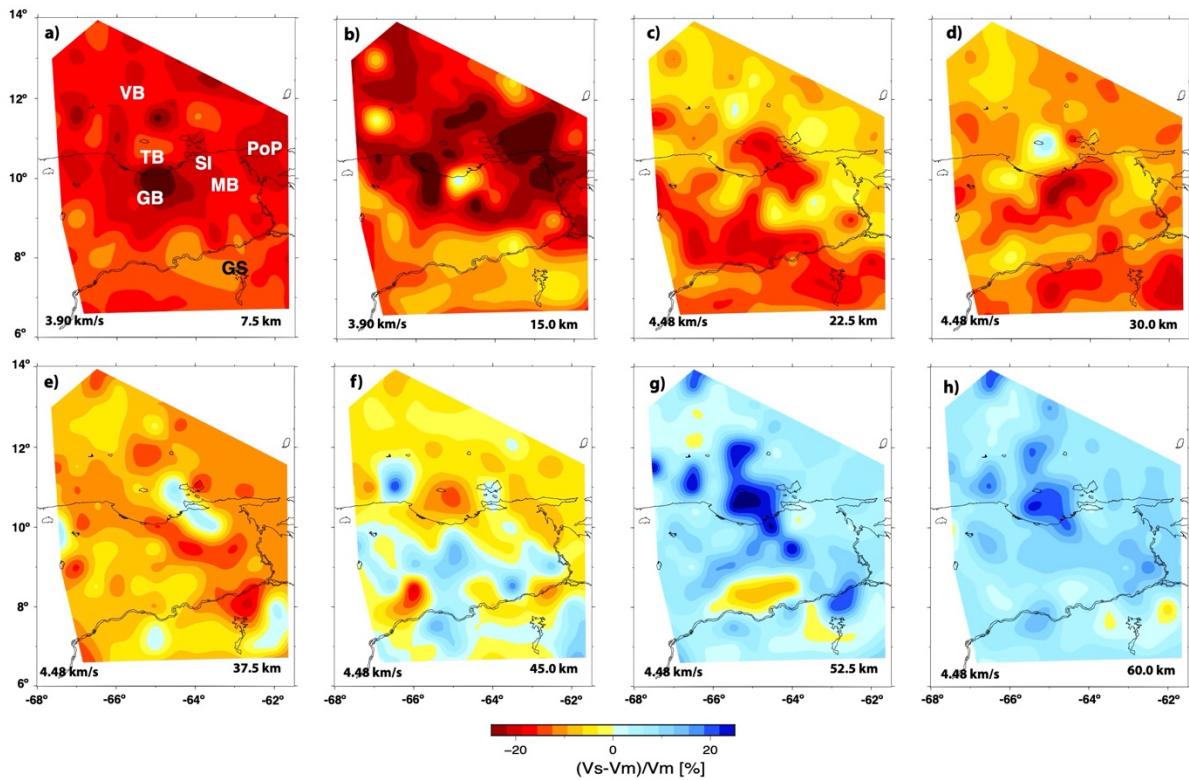


Figure S14. Horizontal slices of the comparison between the global model ak-135-f and the 3D shear wave velocity model of this study. From a) to h) increasing depth in steps of 7.5 km until 60 km depth. In the bottom left is indicated the reference average velocity of the 1-D global model (V_m) and in the bottom right the reference depth. Abbreviations: VB (Venezuela Basin), GS (Guayana Shield), MB (Maturin Basin), GB (Guarico Basin), SI (Serrania del Interior), TB (Turtle the Island-Barcelona Bay) and PoP (Peninsula of Paria).

References

Barmin, M. P., Ritzwoller, M. H., and Levshin, A. L. (2001). A fast and reliable method for surface wave tomography. *Pure and Applied Geophysics*, 158(8), 1351–1375.

Goutorbe, B., de Oliveira Coelho, D. L., & Drouet, S. (2015). Rayleigh wave group velocities at periods of 6–23 s across Brazil from ambient noise tomography. *Geophysical Journal International*, 203(2), 869–882.

Kennett B.L.N., E.R. Engdahl and R. Buland. 1995. “Constraints on seismic velocities in the earth from travel times” *Geophys. J. Int.* 122, 108–124. <https://doi.org/10.1111/j.1365-246X.1995.tb03540.x>